한국퍼지 및 지능 시스템학회 논문지 1998, Vol. 8, No. 4. (1998) 1~7

Meshless Finite Element Analysis of Three-Dimensional Problems Using Fuzzy Knowledge Processing

Joon-Seong Lee

Department of Mechanical Engineering, Kyonggi University

ABSTRACT

This paper describes a meshless of element-free method based on fuzzy knowledge processing. To efficiently simulate complicated physical phenomena with dynamics and non-linear ploblem using computational mechanics, special method is required such as parallel processing or adaptive analysis techniques. However, the conventional finite element method is too complicated to be employed in the above cases. In order to reduce the above complexity of the conventional finite element analysis systems, the so called meshless finite element methods, which do not require connectivity between nodes and elements as an input information have been stuided. Node is generated if its distance from existing node points is similar to the node spacing function at the point. The node spacing function is well controlled by the fuzzy knowledge processing. Practical performances of the present system are demonstrated through several three-dimensional(3D) problems.

1. Introduction

The finite element method (FEM) has been widely utilized in simulating various engineering problems such as structural deformation, thermal conduction, fluid dynamics, electromagnetics and so on. The main reason for this is its high capability of dealing with boundary-value problems in arbitrarily shaped domains. On the other hand, a mesh used influences computational accuracy as well as time so significantly that the mesh generation process is as much important as the FEM analysis itself. Especially, in such large scale nonlinear FEM analyses that approach the limitation of computational capability of so-called supercomputers, it is highly demanded to optimize the distribution of mesh size under the condition of limited total degrees of freedom (DOFs). Thus, the mesh generation process becomes more and more time-consuming and heavier tasks.

Loads for pre-processing and post-processing are increasing rapidly in accordance with an increase of scale and complexity of analysis models to be solved. Particularly, the mesh generation process, which influences computational accuracy as efficiency and whose fully automation is very difficult in 3D cases, has becorne the most critical issue in a whole process of the finite element analyses. In this respect, various researches[1-13] have been performed on the development of automatic mesh generation techniques. However, in reality, general automatic mesh generation techniques have many limitations and concealed experienced know-hows. And general procedure for 3D complex geometries has not been developed yet.

In another approach, meshless method, which do not require mesh subdivisions[14,15], are thought to be effective, since only nodal data is necessary. It will make it easy to handle CAD data. Moreover, because element subdivision processes become unnecessary, adaptive method is expected to be realized easily. If such techniques are established, they will be utilized as the core techniques for realizing CAD/CAE seamless system from modeling to analysis.

The individual techniques in the present study are adopted the practical geometric modelers and the fuzzy knowledge processing. The present systems are constructed in one of popular engineering workstations (EWS) using the C language under the Unix environ- ment.

In the following sections, the fundamental principle of the present algorithm is described. Finally, practical performances of the developed systems are demonstrated through several 3D problems.

2. Outline of the System

2.1 Definition of Geometric Model

Geometric modelers are utilized to define geometries of analysis domains. One of commercial geometric modelers, Designbase[16] is employed for 3D structures. The advantage of Designbase is that a wide range of solid shapes from polyhedra to free-form surfaces can be designed in a unified manner. In these modelers, 3D geometric data are stored as a tree structure of domain-surfaces (free-form surfaces such as Bezier or Gregory type surfaces)-edge (B-spline or Bezier type curves)-vertices.

2.2 Designation of Node Density Distributions

In this section, the connecting process of locally-optimum mesh images is dealt with using the fuzzy knowledge processing technique[17]. In the present system, nodes are first generated. In general, it is not so easy to well control size for a complex geometry. A node density distribution over a whole geometry model is constructed as follows. The present system stores several local nodal patterns such as the pattern suitable to well capture stress concentration, the pattern to subdivide a finite domain uniformly, and the pattern to subdivide a whole domain uniformly. A user selects some of those local nodal patterns, depending on their analysis purposes, and designates where to locate them.

For example, when either the crack of the hole exists solely in an infinite domain, the local node patterns as shown in Figs. 1(a) and 1(b) may be regarded locally-optimum around the crack tip or the hole, respectively. When these stress concentration fields exist closely to each other in the same analysis domain, a simple superposition of both local node patterns gives the result as shown in Fig. 2(b). Namely, extra nodes have to be removed from the superposed region of both patterns.

In the present method, the field A close to the hole and the field B close to the crack-tip are defined in terms of the membership functions used in the fuzzy set theory as shown in Fig. 2(c). For the purpose of

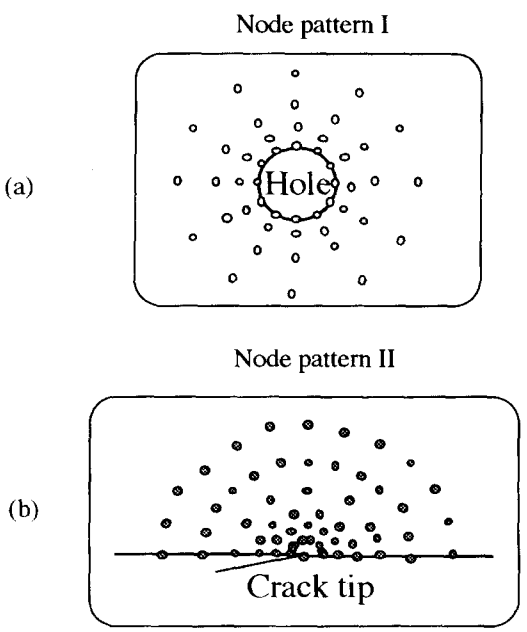

Fig. 1. Example of local node patterns.

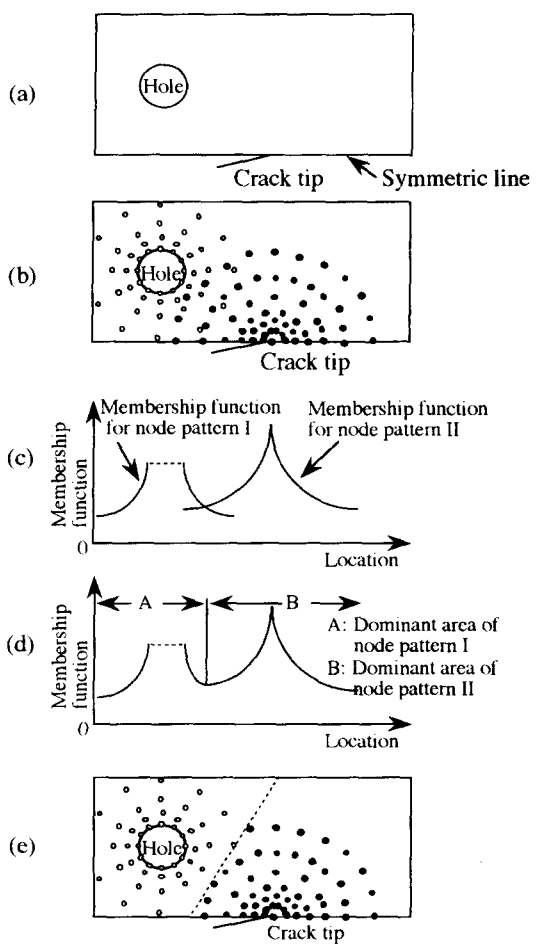

Fig. 2. Superposition of node patterns based on fuzzy theory.

simplicity, each membership function is given a function of one-dimension in the figure. In practice the membership function can be expressed as $\mu(x, y)$ in this particular example, and in 3D cases it is a function of 3D coordinates, i.e. $\mu(x, y, z)$. In Fig. 2(c), the horizontal axis denotes the location, while the vertical axis does the value of membership function, which indicates the magnitude of "closeness" of the location to each stress concentration field. That is, a nodal location closer to the stress concentration field takes a larger value of the membership function. As for Figs. 2(b) and 2(c), choosing the mesh pattern with a larger value of the membership function in each location, one can obtain an overlapped curve of both membership functions, and the domain can be automatically divided into the following two sub-domains A and B as shown in Fig. 2(d) : the sub-domain close to the crack-tip and that of the hole. Finally, both node patterns are smoothly connected as shown in Fig. 2(e). This procedure of node generation, i.e. the connection procedure of both node patterns, is summarized as follows :

• If $\mu_A(x_p, y_p) \geq \mu_B(x_p, y_p)$ for a node p (x_p, y_p) belonging to the pattern A, then the node p is generated, and otherwise p is not generated.

• If $\mu_B(x_q, y_q) \geq \mu_A(x_q, y_q)$ for a node q (x_q, y_q) belonging to the pattern B, then the node q is generated, and otherwise q is not generated.

It is apparent that the above algorithm can be easily extended to 3D problems and any number of node patterns. In addition, since finer node patterns are generally required to place near stress concentration sources, it is convenient to let the membership function correspond to node density as well. According to this definition, Fig. 2(d) also indicates the distribution of node density over the whole analysis domain including the two stress concentration fields.

2.3 Basic algorithm of meshless method

Fig. 3 shows a basic idea of meshless method as an example without any loss of generality. On each node prepared in the domain beforehand, temporary triangular elements are first created by using the node *l*, which is called as a central node, and its surrounding nodes *m, n, o, p*, ..., called as satellite nodes. In the 3D

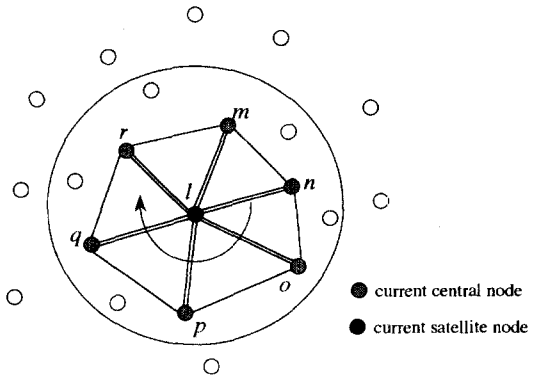

Fig. 3. Temporary triangular elements around node *l*.

solid case, a hexahedron is utilized. On each temporary element, an element matrix is calculated in the next. Third, only the row components of the element matrix, which relate to the central node, are added to the pertinent row of the total stiffness matrix.

More precisely, the satellite nodes *m, n, o, p*, ..., for the central node *l* are first selected. Second, these selected satellite nodes are sorted by clock-wise (or counter clock wise) order with m, say, being the starting node. Third, temporary triangles such as *l-m-n, l-n-o, l-o-p*, ..., are created by using the central node *l* and two neighbouring nodes such as *m-n, n-o, o-p*, ..., respectively. The contribution to the total stiffness matrix is calculated from these triangular temporary elements. For example, and element matrix $[k]_{lnm}$ is calculated from the triangle *l-m-n*, and the node *l* row components of the element matrix $[k]_{lnm}$ are added to the node l row components of the total stiffness matrix. This process is performed throughout all the elements around the node *l*.

It is noted that, in this algorithm, the total stiffness matrix can be evaluated in parallel with respect to each node, and only information about the satellite nodes around the central node is required with each nodal calculation. Therefore, the calculation has an excellent feature of locality of data reference, and then it is considered to be suitable for distributed parallel processing. It is also noteworthy that the cumbersome mesh generation process is avoided. The solution process of the linear equation with the total stiffness matrix can be performed using one of the parallel linear equation solvers such as parallel direct solvers. In the present method, the selection process

of satellite nodes is necessary to be performed instead of the conventional mesh eneration process. This process can be performed efficiently on any distributed parallel processing environment.

2.4 Selection Algorithm of Satellite Nodes

The selection process of the satellite nodes may have strong influence of the accuracy of solution and the execution time of analysis. Fig. 4 shows an example of the mismatch in the triangulation processes, which causes the error in the solution : In Fig. 4(a), the triangle *l-m-o* may be adopted with calculation of the central node *l*, while, in Fig. 2(b), another triangle *o-l-n* with calculation of the central node *o*. As is well known, the total stiffness matrix thus obtained becomes non-symmetric, which leads to erroneous solution. Therefore, the selection process of the satellite nodes should be such that the manners of the triangulations are always as same as possible. If it is the case, the solution of the present method becomes equal to that of the conventional finite element method.

In this context, an algorithm for the optimized selection of the satellite nodes is proposed. The basic idea is very simple and given as follows. Let us take a polygon *l-m-n-o* in Fig. 4. If the length of segment *l-n* is shorter than that of *m-o*, then the node n is taken as a satellite node for the central node *l* and triangles *l-m-n* and *l-n-o* are adopted. If it is not the case, the node n is temporarily deleted and triangle *l-m-o* is adopted. This algorithm is summarized in a systematic manner as follows.

(a) A set of nodes around the central node *l* are selected roughly as candidates of the satellite nodes. For example, the candidate nodes are selected in such a manner that they are within the circle, whose center is located at the central node *l* and the radius of the circle is a function of the node density at the central node.

(b) Segments made of any possible pairs out of candidate nodes *m, n, o, p, ...*, such as *m-o, m-p, n-p, ...*, are sorted by the order of their length as shown in Fig. 5(a).

(c) Starting from the shortest segment, the following process is performed throughout all the segments above. Let's take the segment *m-p* for example, where candidate nodes n and o are located outside from the segment as shown in Fig. 5(b). Whether the nodes *n* and *o* are selected as the satellite nodes or not depends on the relation between the length of the segment *m-p* and the distances from the central node *l* to the candidate node *n* and *o*, respectively. If the segment length *m-p* is longer than that of *l-n*, the node n is taken as a satellite one, and vise versa. The node o is similarly examined.

(d) After a set of the satellite nodes around the node *l* are decided by the above process out of the candidate nodes, a set of triangles are created in a radial topology using the satellite nodes with the central node *l* being the common node as shown in Fig. 1. Then, the calculation of element matrices and assemble process into the total stiffness matrix are performed according to the method described in the previous section.

(e) The process from (a) through (d) above are performed throughout the nodes in the domain.

3. Examples

The present method was applied to two-dimensio-

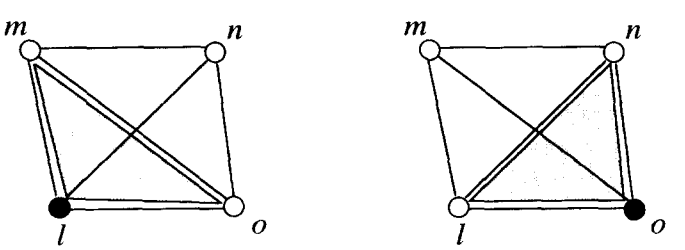

(a) the case when *l* being a central node (b) the case when *o* being a central node

Fig. 4. Mismatch in triangulation processes.

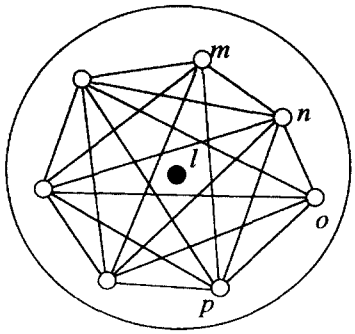

(a) complete set of diagonal segments

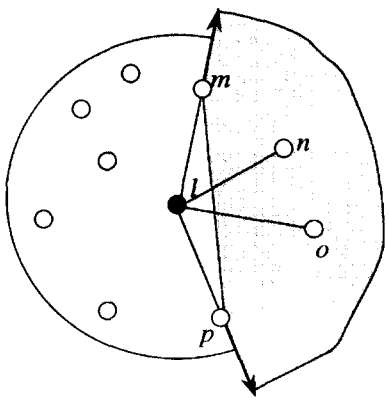

(b) nodes n and o outside diagonal segment m-p

Fig. 5. Selection algorithm of satellite nodes.

nal static heat conduction problem to show the performance and accuracy. Fig. 6 shows the analysis domain and the conditions. Table 1 shows the comparisons of temperature values obtained at four points A, B, C and D along the top edge of the domain between the present method and the conventional method. Here, the conventional method means the finite element method with the mesh using the Delaunay triangulation. The present method employs the same nodal pattern as in the above Delaunay triangulation.

Applying the present scheme to the nodal pattern shown in Fig. 7, it is shown that no mismatch of triangles occurs. This means that a mesh for this domain is created implicitly by this method and that the small difference between the present solution and that of the Delaunay mesh attributes to the difference of the mesh topology seen at a few parts of the domain between the two methods.

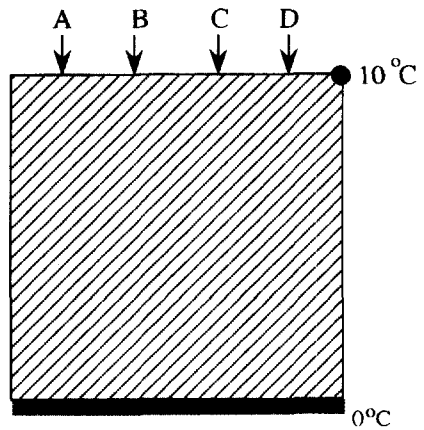

Fig. 6. Analysis shape and analysis conditions.

As an example of the three-dimensional solid analysis, a transient heat conduction problem was analyzed. The temperature of a piston head, as shown in Fig. 8, was initially set 100°C throughout. Top face and outer face of the piston head had a temperature of 0°C. The other faces were insulated. The temperature of the piston head was calculated for subsequent times (0 to 10 secs). In this problem, material properties selected were : thermal conductivity of 1.0 J/(m · s · °C), specific heat of 1.0 J/(kg · °C) and mass density of 1.0 kg/m^3.

Table 1. Analysis result for temperature at A, B, C and D

Location	Conventional FEM	Present
A	1.450043	1.450019
B	2.048639	2.048665
C	3.681370	3.681408
D	7.537236	7.537259

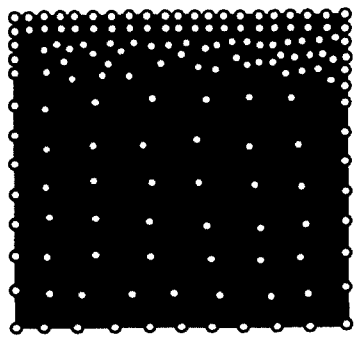

Fig. 7. Nodal pattern.

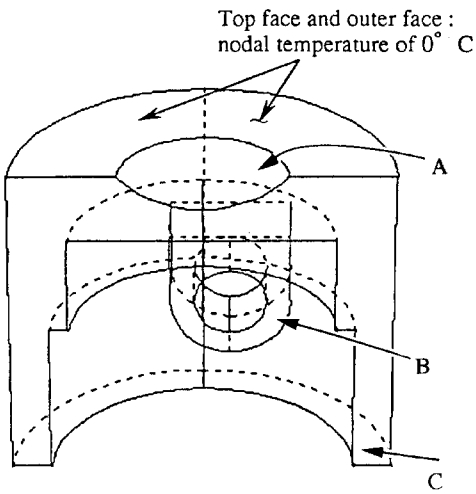

Fig. 8. Geometry model of piston head.

The initial temperature at all nodes was 100°C. At time t=0, top and outer face have a prescribed temperature of 0°C ; all other surfaces are adiabatic and require no data input. A transient solution is performed with 10 uniform time steps of 0.1 seconds each for a total time of 1 second.

Fig. 9 shows an appearance of nodes. Also, the present method employs the same nodal pattern as in the Delaunay triangulation. In order to show the performance of the present method, one of commercial finite element analysis codes is used. Fig. 10(a) and (b) show a calculated distribution of temperature at 0.3 and 1 second, respectively. Table 2 shows the comparisons of temperature values obtained at three points A, B, and C of the piston

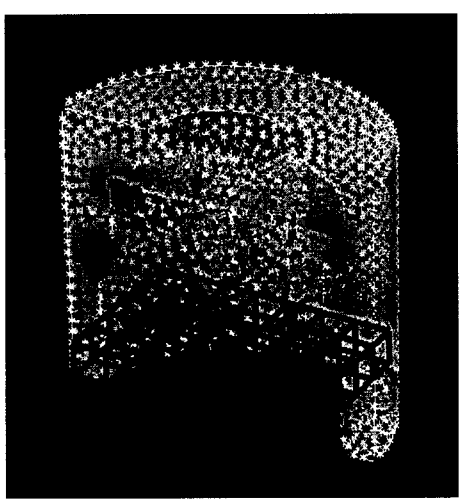

Fig. 9. Appearance of node generation.

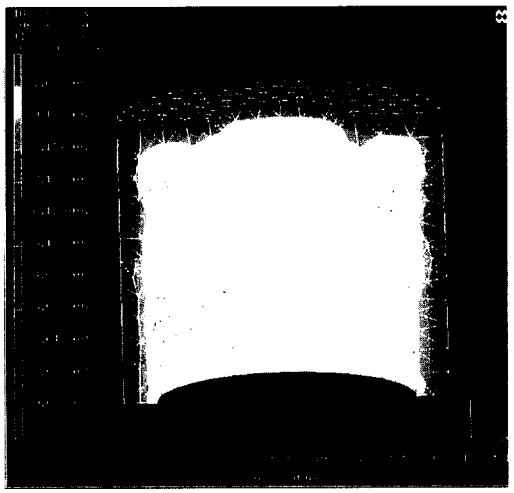

(a) at 0.3 sec

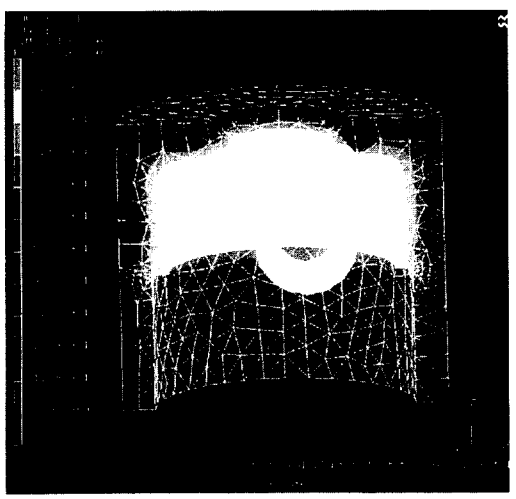

(b) at 1 sec

Fig. 10. Distribution of temperature.

Table 2. Analysis result for temperature at A, B and C

Time	Location	Conventional FEM	Present
0.3 sec	A	92.9432	92.9431
	B	97.3983	97.9981
	C	78.3984	78.3986
1.0 sec	A	74.9867	74.9899
	B	99.9999	99.9878
	C	43.4982	43.4911

domain between the present method and the commercial finite element analysis code. It can be seen from the table that the present methods agree well with the conventional methods within 2 to 3% difference.

4. Conclusions

In this paper, a novel type of meshless finite element method, which does not require connectivity information between elements and nodes. In this method, a set of triangular or tetrahedral elements are temporarily created around each node, then the total stiffness matrix is obrained by adding the row components of the temporary element matrices to the relevant row components of the total stiffness matrix.

It is shwon that nearly the same solution as the conventional finite element method using the Delaunay mesh is obtained under the condition of complicated distribution pattern of nodes. In this regard, the present method could be employed as a new mesh generation technique.

REFERENCES

[1] Watson, D.F., "Computing The N-Dimensional Delaunay Tessellation with Application to Voronoi Polytopes," The Computer Journal, **24**(2), pp. 167-172, 1981.

[2] Schroeder, W.J. and Shephard, M.S., "Combined Octree/Delaunay Method for Fully Automatic 3-D Mesh Generation," International Journal for Numerical Methods in Engineering, **29**, pp. 37-55, 1990.

[3] Lee. D.T. and Schachter, B.J., "Two Algorithms for Constructing a Delaunay Triangulation," International Journal of Computer and Information Sciences, **9**(3), pp. 219-242, 1980.

[4] Shephard, M.S., Yerry, M.A. and Baehmann, L., "Automatic Mesh Generation Allowing for Efficient a Priori and a Posteriori Mesh Refinement," Computer Methods in Applied Mechanics and Engineering, **55**, pp. 161-180, 1986.

[5] Buratynski, E.K., "Fully Automatic Three-Dimensional Mesh Generator for Complex Geometries," International Journal for Numerical Methods in Engineering, **30**, pp. 931-952, 1990.

[6] Pourazady, M. and Radhakrishnan, M., "Optimization of a Triangular Mesh," Computers and Structures, **40**(3), pp. 795-804, 1991.

[7] Bowyer, A., "Computing Dirichlet Tessellations," The Computer Journal, **24**(2), pp. 162-172, 1981.

[8] Shephard, M.S. and Georges, M.K., "Automatic Three-Dimensional Mesh Generation by the Finite Octree Technique," International Journal for Numerical Methods in Engineering, **32**, pp. 709-749, 1991.

[9] Sezer, L. and Zeid, I., "Automatic Quadrilateral/Triangular Free-Form Mesh Generation For Planar Regions," International Journal for Numerical Methods in Engineering, **32**, pp. 1441-1483, 1991.

[10] Al-Nasra, M. and Nguyen, D.T., "An Algorithm for Domain Decomposition in Finite Element Analysis," Computers and Structures, **39**(3/4), pp. 277-289, 1981.

[11] Green, P.J. and Sibson, R., "Computing Dirichlet Tessellations in The Planes," The Computer Journal, **21**(2), pp. 168-173, 1977.

[12] Taniguchi, T. and Ohta, C., "Delaunay-Based Grid Generation for 3D Body with Complex Boundary Geometry," Grid Generation Conference, 1991.

[13] Sloan, S.W., "Fast Algorithm for Constructing Delaunay Triangulation in the Plane," Advanced Engineering Software, **9**(1), pp. 34-55, 1987.

[14] Belytschko, T., Lu, Y.Y. and Gu, L., "Element-Free Galerkin Methods," International Journal of Numerical Methods in Engineering, **37**, pp. 229-256, 1994.

[15] Nayroles, B., Touzot, G. and Villon, P., "Generating the Finite Element Method : Diffuse Approximation and Diffuse Elements," Computational Mechanics, **10**, pp. 307-318, 1992.

[16] Chiyokura, H., Solid Modeling with Designbase : Theory and Implementation, Addition-Wesley, 1988.

[17] Joon-Seong Lee, "Automated CAE System for Three-Dimensional Complex Geometry," Doctoral Dissertation, Faculty of Engineering, The University of Tokyo, 1995.

이 준 성(Joon-Seong Lee)

1986년 : 성균관대학교 기계공학과 학사
1988년 : 동대학원 기계공학과 석사
1988년~1991년 : 육군사관학교 기계공학과 교수
1991년~1992년 : KIST 연구원
1995년 동경대학 공학박사
1996년~현재 : 경기대학교 기계공학과 조교수

관심분야 : 계산역학, 구조물의 자동설계, 지적 시뮬레이션